Proc. Natl. Acad. Sci. USA
Vol. 91, pp. 6629–6633, July 1994
Neurobiology

Two-photon scanning photochemical microscopy: Mapping ligand-gated ion channel distributions

(caged compounds/voltage-clamp/synaptic connections)

WINFRIED DENK

AT&T Bell Laboratories, Murray Hill, NJ 07974

Communicated by George P. Hess, March 11, 1994

ABSTRACT **The locations and densities of ionotropic membrane receptors, which are responsible for receiving synaptic transmission throughout the nervous system, are of prime importance in understanding the function of neural circuits. It is shown that the highly localized liberation of "caged" neurotransmitters by two-photon absorption-mediated photoactivation can be used in conjunction with recording the induced whole-cell current to determine the distribution of ligand-gated ion channels. The technique is potentially sensitive enough to detect individual channels with diffraction-limited spatial resolution. Images of the distribution of nicotinic acetylcholine receptors on cultured BC3H1 cells were obtained using a photoactivatable precursor of the nicotinic agonist carbamoylcholine.**

Knowledge of the synaptic connectivity, which is closely reflected in the distribution of postsynaptic receptors, is central to the understanding of how computation is performed in the nervous system. Much effort has been expended to characterize ligand-gated ion channels in terms of their molecular, kinetic, and pharmacological properties (1). Receptor distributions have been studied with the help of labeled antagonists, toxins, or antibodies (2–4) and by iontophoretic mapping (5, 6). Two-photon scanning photochemical microscopy (TPSPM) with whole-cell current detection, as introduced in this report, allows one to determine the distribution of neurotransmitter-gated ion channels on a chosen cell with a resolution approaching the optical diffraction limit in all three spatial dimensions.

The principle behind TPSPM (Fig. 1) is to generate a high concentration of agonist in a small volume by localized photolysis of a bath-applied photoactivatable or caged agonist (CA) (7, 8). If this volume is adjacent to ionotropic cell membrane receptors for that particular agonist the corresponding ion channels open, in turn admitting a current whose magnitude reflects the number of activated receptors at that particular location. The position of the focus of the uncaging laser beam and with it the location of high agonist concentration is scanned across the cell under investigation and the whole-cell current is recorded (9) at the same time. The observed current magnitude is used to control the darkening of the corresponding pixel. The resulting "photoactivated" current (I_{pa}) image reflects the receptor distribution on the cell (see Fig. 2). TPSPM is much faster (Fig. 2*b* was acquired in just over 2 min) than iontophoretic mapping, does not require mechanical access for an iontophoresis pipette, and does not generate ejection-current artifacts. In TPSPM, unlike with binding assays, receptors stay functional and only functional receptors are detected.

The use of pulsed red or infrared light in conjunction with simultaneous two-photon absorption to release CA instead of using single-photon absorption at ultraviolet wavelengths (10, 11) has several advantages (12–14). The optical *resolution*—i.e., the smallness of the region of largest excitation—is generally not improved (13) by using two-photon excitation since the increase in the size of the diffraction-limited focal spot by using twice the wavelength of one-photon excitation is only partially compensated for by the sharpening due to the nonlinear absorption (for Gaussian beams the loss in resolution is $\sqrt{2}$). But the optical *localization*—i.e., the speed with which the excitation falls off with distance from the focal point—is dramatically improved due to the quadratic dependence of the absorption probability on the light intensity in combination with the strong focusing of the uncaging beam (Fig. 1), which confines the majority of all excitations to a volume of <1 fl (1 μm^3) around the focal point. The resulting background rejection is indispensable in photoactivation applications since, unlike in fluorescence- or backscattering microscopy, no additional spatial localization and discrimination can be achieved by spatially filtering the elicited signal. Such spatial filtering is, however, the basis for the optical sectioning properties of the one-photon confocal microscope (15). Major agonist release outside the focal plane, inevitable under one-photon excitation, does not occur with two-photon excitation (12). Thereby one avoids (*i*) blurring of the image as in nonconfocal fluorescence microscopy, (*ii*) activation of background current with its associated channel-gating noise, (*iii*) global receptor desensitization, and (*iv*) depletion of the supply of CA. Other advantages are reduced out-of-focus photodamage (see below) and improved depth penetration in thick specimens due to lack of out-of-focus (inner) absorption (16) by the CA itself and due to greatly reduced scattering at longer wavelengths (17).

MATERIAL AND METHODS

To achieve a sufficient rate of two-photon absorption at tolerable average power levels ultrashort pulses have to be used (12). I used the output from a colliding pulse mode-locked dye laser (18) with rhodamine B as a gain medium and 3,3′-diethyloxacarbocyanine iodide as a saturable absorber providing pulses with a pulse length below 100 fs at a repetition rate of 150 MHz and an average power of about 50 mW, of which about 18 mW reached the sample. Rhodamine B rather than the originally (18) used rhodamine 6G was chosen as gain dye since that resulted in a lasing spectrum shifted to slightly longer wavelengths, centered at 640 nm.

The laser beam was focused to a diffraction limited spot using a 40×/1.3 numerical aperature objective lens (Plan Neofluar; Zeiss) while scanning was performed using a laser scanning microscope (MRC600; Bio-Rad) that was modified as follows: scan mirrors were brought into close proximity, with the intervening optics removed; the eyepiece was re-

The publication costs of this article were defrayed in part by page charge payment. This article must therefore be hereby marked "*advertisement*" in accordance with 18 U.S.C. §1734 solely to indicate this fact.

Abbreviations: TPSPM, two-photon scanning photochemical microscopy; CA, caged agonist; I_{pa}, photoactivated current; nAChR, nicotinic acetylcholine receptor.

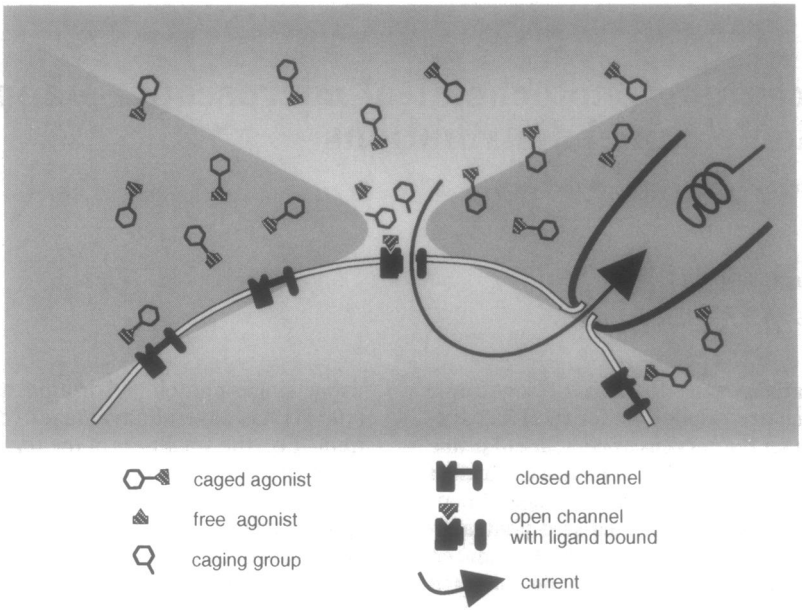

FIG. 1. Illustration of the principle of TPSPM with whole-cell current detection. Agonist is released, after two-photon absorption, from a "caged" precursor only in the focal region of the highly focused laser beam (shaded double cone) and then binds to nearby receptors. Correspondingly activated channels then allow the flow of an ionic current across the cell membrane. The current is then detected with a patch-clamp electrode operating in the whole-cell configuration.

placed by an achromatic doublet (f = 80 mm) to reduce the effective separation of the scan mirrors at the objective's rear focal plane; the signals controlling mirror deflections and data acquisition were generated using custom software and an additional analog interface board because the original instrument allowed neither slow enough scan speeds nor random scanning.

Whole-cell recordings were made using standard techniques (9). The solution inside the recording pipette contained potassium methanesulfonate (120 mM), Hepes (5 mM), EGTA (10 mM), and $MgCl_2$ (2 mM). Pipettes were pulled from borosilicate glass capillaries, slightly heat polished, and had resistances of 5–7 MΩ, yielding access resistances of 7–12 MΩ. At the −60 mV holding potential, which was used throughout, the seal leakage currents were typically <10 pA and the whole-cell holding currents were <25 pA just after establishing whole-cell recording conditions by applying a suction transient. All experiments were done at room temperature. Cells were bathed in Dulbecco's modified eagle medium (DMEM) (Sigma) lacking phenol red but with the addition of Hepes buffer (25 mM) and sodium bicarbonate (10 mM) with the addition of free or CA as indicated. The pH of all solutions was adjusted to 7.3. Caged carbamoylcholine {*N*-[(α-carboxy)-2-nitrobenzyl]carbamoylcholine trifluoroacetate; Molecular Probes} was purified before use on a reverse-phase HPLC column (Deltapack; Waters) largely as described (19).

The cell line was maintained in tissue culture flasks in DMEM with 10% fetal bovine serum (FBS; Sigma) and passed once a week. Cells for measurements were plated on glass coverslips cleaned in a freshly prepared mixture of 70% H_2SO_4/30% H_2O_2 and maintained in DMEM with 1% FBS for at least a week to promote differentiation and expression of functional receptors (20) before recording.

RESULTS

In the brain's intertwined network of cellular processes binding studies using labeled ligands often do not allow the assignment of receptors to a particular cell. This is a severe drawback if specific connections are to be traced. TPSPM, on the other hand, specifically detects receptors on the one cell that was selected for whole-cell recording. Single-cell specificity is illustrated in Fig. 2 by the lack of response along the perimeter of a neighboring cell. The voltage-clamped cell in the center of Fig. 2 shows an I_{pa} distribution, with receptors all along the cell's perimeter, that was typical for most of the >40 cells, from a nonfusing muscle cell line (20, 22) (BC3H1), that were studied. The "bright" interior of the cell, indicating the absence of current activation, shows that only receptors in the optical slice around the focal plane are activated and provides evidence for the optical sectioning properties of TPSPM. The I_{pa} distribution is found to be essentially independent of the direction of scanning (compare Fig. 2 *b* and *c*, and see below).

The optical sectioning properties are apparent in a sequence of TPSPM scans (Fig. 3) taken at different positions of the focal plane with respect to the coverslip surface. Note,

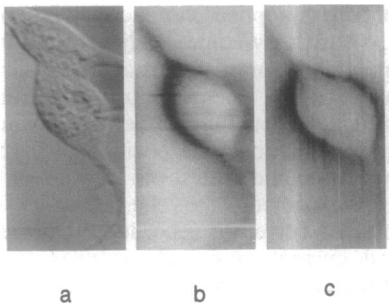

FIG. 2. Raster scanned images of cultured BC3H1 cells. (*a*) Beam deflection image (21), which provides Nomarski-like contrast. (*b* and *c*) Nicotinic acetylcholine receptors (nAChRs) imaged with TPSPM and whole-cell current detection (inward displayed as darkening). Bathing medium with 0.5 mM caged carbamoylcholine (CA) was perfused over the cell from the lower left direction using a 200-mm i.d. capillary (not visible). *a* and *b* were scanned with horizontally oriented and *c* with vertically oriented lines; scans started in both cases at the upper left corner of the image. The pixel dwell time was 6.8 ms. The cell in this image had a cell capacitance of 31.5 pF and an access resistance of 10.5 MΩ and was used on day 7 after plating. The holding current was increased to 270 pA with CA (see text). Image size: 100 × 200 pixels corresponding to 50 μm × 100 μm.

in particular, how photolysis-induced signals suddenly appear in the second image after being undetectable in the first image where the focal plane was just 0.7 μm below the coverslip surface, on which the cells grew. Including those used to acquire the images shown in Fig. 3, a total of 38 scans was performed across this cell during a period of 90 min after which the whole-cell leakage current (at −60 mV) had increased to 40 pA from an initial value of 7 pA.

Pseudo-random scanning, as shown in Fig. 4*b*, avoids artifacts that are caused by the sequential release of (diffusible) agonist in nearby pixel locations along a scan line. For example (Fig. 2), as the scanned beam approaches the cell membrane from the outside it is accompanied by a diffusive wave of previously released agonist, leading to a larger response than if the beam comes from the inside of the cell, which is devoid of caged precursor and is, in addition, separated by the cell membrane, which acts as a diffusion barrier. Note that Fig. 4 shows significant I_{pa} spots for beam positions seemingly inside the cell. These features were found on several cells and—like the circumferential responses—were suppressed by predesensitization (see below), suggesting that the nAChR distribution extends into membrane invaginations, which are typical for these cells (22).

Appropriately timed acquisition combined with periodic shuttering of the laser beam was used in random scanning and is illustrated in Fig. 5. Photolysis and receptor activation occur on a submillisecond time scale (19, 24). I_{pa} rise times, typically between 5 and 20 ms, are therefore dominated by diffusion times between the release points in the laser focus and the nAChRs. Since nAChRs are present in a relatively low area density on these cells (≈10 per μm^2) recruitment from a considerable membrane area is necessary to amount to a detectable I_{pa}. Sufficient signal in a time window that is short enough to avoid diffusional blurring altogether can be expected for improved CAs that do not activate and desensitize the receptors (see below).

No current was induced by the scanned laser beam without CA or with CA when, to rule out nonspecific effects due to laser light absorption by CA, receptors had been inactivated by predesensitization using a saturating dose of free carbamoylcholine. The maximum I_{pa} in Fig. 2 *b* and *c* was 360 pA, corresponding to about 150 open channels (25). The background noise level with CA was 16 pA_{rms} (in a bandwidth of about 70 Hz as determined by the pixel dwell time) compared with roughly 1.5 pA without CA. Therefore, the dominant current-noise source is the channel gating noise due to dark activation (equivalent to 2–5 mM free carbamoylcholine) by CA itself or by a small amounts of free carbamoylcholine present in spite of HPLC purification (19). A reversible reduction of I_{pa}, consistent with desensitization, was observed if a cell was exposed to CA (500 mM) for extended periods (>10 min).

A potential limitation in all photoactivation experiments is the damage caused by intrinsic absorption of the excitation light. In TPSPM damage due to intrinsic two-photon absorption is, however, expected only in the focal plane and very

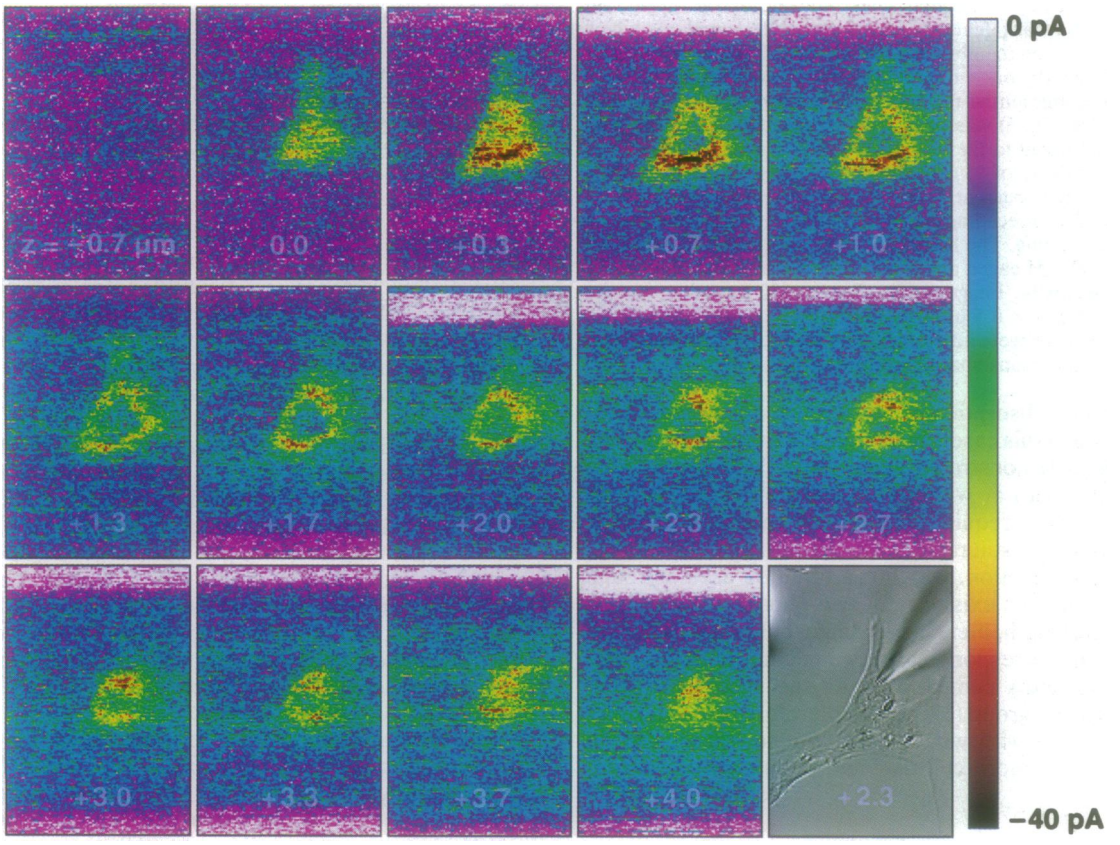

FIG. 3. Optical sectioning properties of TPSPM microscopy as demonstrated by a "through-focus-series" of photoactivated current images. The lack of out-of-focus release of agonist is strikingly evident from the difference between the images taken with the focal plane position (z) 0.7 μm below the coverslip surface and the large amount of induced current seen for z = 0.3 μm. A beam deflection image, taken simultaneously with one of the I_{pa} images, of the cell with the attached recording pipette is shown at an intermediate focal plane position (z = 2.3 μm above coverslip) in the lower left corner. Images were raster-scanned with the fast axis horizontal. Bright stripes visible in the top and/or bottom portions of several images result from the delayed introduction or early withdrawal of the flow of caged compound-containing solution over the cell. The current range displayed is 0 to −40 pA. Recording conditions were very similar to those in Fig. 2. This cell was used on day 7 after plating. The access resistance after establishing whole-cell condition was 12 MΩ and rose to 19 MΩ toward the end of the experiment. The cell capacitance was 24 pF. Image size: 100 × 200 pixels corresponding to 50 μm × 100 μm.

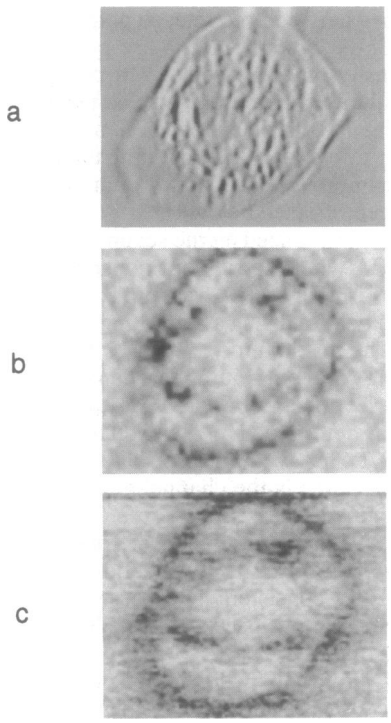

FIG. 4. Comparison of raster scan and pseudo-random scan. Deflection (*a*; ref. 21) and current (*c*) were acquired with conventional scanning using horizontal lines, starting at the upper left corner. Note the dark features inside the cell (*b* and *c*), which represent nAChRs on membrane invaginations. In *b* (current) pixels were visited exactly once in pseudo-random sequence generated using a linear congruential method (23). At each location the laser shutter (see also Fig. 5) was opened for 35 ms after which the scan location was changed to the next pixel in the sequence, which was exposed after a delay of 55 ms. The pixel darkening in *b* is proportional to the average current during the shutter open time minus the current in the 30 ms preceding the shutter opening. This cell was used on day 23 after plating. The holding current increased to 550 pA and 900 pA with 500 mM caged and 5 mM free carbamoylcholine in the medium, respectively. Image size is 47 μm × 32 μm with a square pixel size of 0.5 μm × 0.5 μm for *a* and *c* and 1 μm × 1 μm for *b*. Pixel boundaries in *b* were intentionally blurred to avoid meaningless but visually conspicuous sharp brightness steps.

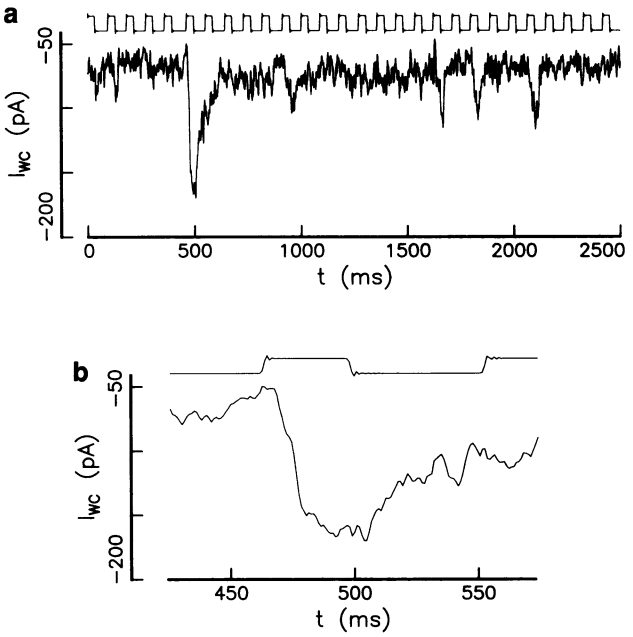

FIG. 5. Whole-cell current (I_{wc}) response to shuttered exposures during random scanning (Fig. 3*b*) is shown together with the shutter drive signal. In *b* part of *a* is displayed on a faster time scale to show the rise time of the whole-cell current at a pixel location that gave one of the largest responses during the acquisition of Fig. 4*b*.

little one-photon absorption occurs at the fundamental wavelength (640 nm in this case). In fact, as the example of the cell shown in Fig. 3 demonstrates, even after repeatedly scanning the same cell—with or without CA—at slow scanning rates (5–10 ms per pixel) required for photochemical imaging the holding current was still rather low. For proteins the intrinsic (one-photon) absorption, which can often be used as rough guidance (12) for the existence of two-photon absorption at twice the wavelength, increases strongly below a wavelength of 300 nm (30) (corresponding to two 600-nm photons). The longest wavelengths compatible with the absorption spectrum of the caging group (19) should therefore be used. Early experiments done with wavelengths around 620 nm did, in fact, cause much more cell damage (unpublished observations).

CONCLUSIONS

The spatial resolution of TPSPM is ultimately limited by the smallest achievable diffraction-limited focus spot (about 0.3 μm wide and 1 μm high), as is generally the case in far field light microscopy. Additional resolution limitations result, however, from the rapid dispersion of the released agonist by diffusion, which blurs the image, particularly if the combined kinetics of agonist release and receptor activation are slow. The CA compound used in the present experiments, *N*-[(α-carboxy)-2-nitrobenzyl]carbamoylcholine, has almost perfect properties for kinetic studies of the nicotinic receptor (19). But even though this compound shows the desired fast photoactivation kinetics it is not ideal for TPSPM because it slightly activates and significantly desensitizes receptors at the concentrations (0.5 mM) that have to be used for TPSPM. Furthermore, no natural removal mechanism exists for free carbamoylcholine that might be present. For caged indigenous transmitters such mechanisms are likely to reduce this source of background significantly, potentially obviating the need for elaborate chemical purification procedures. It is important to be able to use a CA at high concentrations without causing gating noise and desensitization in order to (*i*) achieve the fast activation and good signal-to-noise ratio necessary to avoid diffusional artifacts and (*ii*) be able to release a sufficient number of agonist molecules in spite of the small CA-containing extracellular volume in the constrained geometry of the synaptic cleft. Furthermore, under favorable conditions single-channel currents can be resolved in the whole-cell configuration (9). If dark activation noise, which presently limits the sensitivity, can, therefore, be eliminated through improved chemical caging technology (8) TPSPM may well become sensitive enough to even detect the presence of single receptors in the release volume and hence be at least as sensitive as binding studies using fluorescent, radioactive, or colloidal labels.

The approach described here should be easily expandable to other ligand-gated ion channels. And since the development of photoactivatable probes for biological applications is a rather active field (7, 8, 26) we can expect synthesis of new caged agonists conceivably even with their properties specifically tailored to the needs of TPSPM. In thick preparations of complex tissues—e.g., in brain slices—the unique optical sectioning properties, the reduced photodamage, and the selectivity for receptors on the cell from which one is recording are expected to make two-photon photochemical microscopy the method of choice for receptor localization on the light microscopic level. Another promising application is the localized release, inside cells, of caged second messen-

gers such as inositol 1,4,5-trisphosphate, GMP, or calcium (7, 8, 27–29) to elucidate mechanism of intra- rather than intercellular signaling.

I thank Dr. G. P. Hess for suggesting to use BC3H1 cells and for the gift of the cell line, Drs. L. Niu and A. Mueller for advice on the purification procedure, F. Raccuia-Behling for help in culturing the cells, Jürgen Steyer for improvements in the purification procedure, and Drs. K. Delaney, M. Fee, A. Gelperin, D. Kleinfeld, R. Lobnig, and D. Tank for comments on the manuscript.

1. Hille, B. (1992) *Ionic Channels of Excitable Membranes* (Sinauer, Sunderland, MA).
2. Ravdin, P. & Axelrod, D. (1977) *Anal. Biochem.* **80**, 585–592.
3. Fertuck, H. C. & Salpeter, M. M. (1974) *Proc. Natl. Acad. Sci. USA* **71**, 1376–1378.
4. Veitel, D. & Robenek, H. (1988) *J. Histochem. Cytochem.* **36**, 1295–1303.
5. Dennis, M. J., Harris, A. J. & Kuffler, S. W. (1971) *Proc. R. Soc. London B* **177**, 509–539.
6. Miledi, R. (1960) *J. Physiol. (London)* **151**, 24–30.
7. Kao, J. P. K. & Adams, S. R. (1993) in *Optical Microscopy: Emerging Methods and Applications.*, eds. Herman, B. & Lemasters, J. J. (Academic, San Diego), pp. 27–85.
8. Adams, S. R. & Tsien, R. Y. (1993) *Annu. Rev. Physiol.* **55**, 755–784.
9. Hamill, O. P., Marty, A., Neher, E., Sakmann, N. & Sigworth, F. J. (1981) *Pflügers Arch.* **391**, 85–100.
10. Bliton, C., Lechleiter, J. & Clapham, D. E. (1993) *J. Microsc. (Oxford)* **169**, 15–26.
11. Callaway, E. M. & Katz, L. C. (1993) *Proc. Natl. Acad. Sci. USA* **90**, 7661–7665.
12. Denk, W., Strickler, J. H. & Webb, W. W. (1990) *Science* **248**, 73–76.
13. Sheppard, C. J. R. & Gu, M. (1990) *Optik* **86**, 104–106.
14. Nakamura, K. (1993) *Optik* **93**, 39–42.
15. Wilson, T. & Sheppard, C. (1984) *Theory and Practice of Scanning Optical Microscopy* (Academic, New York).
16. Zucker, R. S. (1992) *Cell Calc.* **13**, 29–40.
17. Wan, S., Parrish, J. A., Anderson, R. R. & Madden, M. (1981) *Photochem. Photobiol.* **34**, 679–681.
18. Valdemanis, J. A. & Fork, R. L. (1986) *IEEE J. Quantum Electron.* **QE-22**, 112.
19. Milburn, T., Matsubara, N., Billington, A. P., Udgaonkar, J. B., Walker, J. W., Carpenter, B. K., Webb, W. W., Marque, J., Deuk, W., McCray, J. A. & Hess, G. P. (1989) *Biochemistry* **28**, 49–55.
20. Patrick, J., McMillan, J., Wolfson, H. & O'Brian, J. C. (1977) *J. Biol. Chem.* **252**, 2143–2153.
21. Wilson, T. (1987) *Optik* **80**, 167–170.
22. Schubert, D., Harris, A. J., Devine, C. E. & Heinemann, S. (1974) *J. Cell. Biol.* **61**, 398–413.
23. Press, W. H., Flannery, B. P., Teukolsky, S. A. & Vetterling, W. T. (1988) *Numerical Recipes in C* (Cambridge Univ. Press, Cambridge, U.K.).
24. Matsubara, N., Billington, A. P. & Hess, G. P. (1992) *Biochemistry* **31**, 5507–5514.
25. Sine, S. M. & Steinbach, J. H. (1984) *Biophys. J.* **45**, 175–185.
26. Corrie, J. E. T. & Trentham, D. R. (1993) in *Bioorganic Photochemistry*, ed. Morrison, H. (Wiley, New York), Vol. 2.
27. Tsien, R. Y. & Zucker, R. S. (1986) *Biophys. J.* **50**, 843–853.
28. Karpen, J. W., Zimmerman, A. L., Stryer, L. & Baylor, D. A. (1988) *Proc. Natl. Acad. Sci. USA* **85**, 1287–1291.
29. Kaplan, J. H. & Ellis-Davies, G. C. R. (1988) *Proc. Natl. Acad. Sci. USA* **85**, 6571–6575.
30. Rehms, A. D. & Callis, P. R. (1993) *Chem. Phys. Lett.* **208**, 276–282.